First-principles study of elastic properties of Cr- and Fe-rich Fe-Cr alloys

Vsevolod I. Razumovskiy,* Andrei V. Ruban, and Pavel A. Korzhavyi
Applied Materials Physics, Department of Materials Science and Engineering, Royal Institute of Technology, SE-100 44 Stockholm, Sweden

(Received 8 February 2011; revised manuscript received 28 April 2011; published 5 July 2011)

Elastic properties of substitutionally disordered Cr- and Fe-rich Fe-Cr alloys are derived from first-principles calculations using the exact muffin-tin orbitals method and the coherent potential approximation. A peculiarity in the concentration dependence of elastic constants in Fe-rich alloys is demonstrated and related to a change in the Fermi surface topology. Our calculations predict high values for the elastic constants of Cr-rich Fe-Cr alloys, but at the same time show that these alloys could be rather brittle according to the Pugh criterion (the ratio between shear and bulk moduli is calculated to be greater than 0.5).

DOI: 10.1103/PhysRevB.84.024106 PACS number(s): 62.20.D−, 31.15.A−, 71.20.Be

I. INTRODUCTION

Fe-Cr alloys are the base for a wide range of materials, from steels to superalloys. The Fe-rich Fe-Cr alloys are of primary interest for the stainless-steel industry, whereas the Cr-rich alloys are of importance for high-temperature applications. The most attention has recently been drawn to the problems of stainless steels because of their potential applications as construction materials for nuclear fission and fusion reactors.[1] Alloys from the middle of the Fe-Cr binary system undergo a decomposition onto the mixture of Cr- and Fe-rich alloy fractions at temperatures below about 800 K.[2] Therefore, detailed knowledge about the properties of these two terminal compositional regions of the Fe-Cr system is of primary practical importance.

At first sight, the elastic properties of this system seem to be quite well established from both experimental[3–12] and theoretical[13–18] points of view. However, there are many complicated features of this system on both Fe- and Cr-rich sides. In pure chromium and chromium-rich alloys, the spin-density-wave (SDW) antiferromagnetic ordering[19] affects many physical properties, including elastic properties, and their investigation thus requires the use of elaborate theoretical tools. In the Fe-rich Fe-Cr alloys, a peculiarity has been noted[3,20] in the concentration dependence of the bulk modulus at around 6 at.% Cr, which is probably related to the Fermi surface topology change that occurs near the same composition.[21] Whether or not the change of Fermi surface topology has an effect on the elastic properties of the Fe-rich Fe-Cr alloys is the main question that will be addressed in this paper. Also, the results of our first-principles investigation of the elastic properties of Cr-rich Fe-Cr random alloys will be presented.

II. METHODOLOGY

A. Electronic structure calculations

The present electronic structure calculations of Fe-Cr alloys are based on density functional theory[22] (DFT) and have been performed by means of the exact muffin-tin orbitals (EMTO) method.[23–25] Substitutional disorder in the body-centered-cubic (bcc) Fe-Cr alloys is treated within the coherent potential approximation (CPA).[26] In this case, additional contributions to the one-electron potentials of alloy components and the total energy should be taken into consideration in the single-site DFT formalism.[27] The screening contributions to the on-site electrostatic potential $V^i_{\rm scr}$ and electrostatic energy $E_{\rm scr}$ are determined as[27]

$$V_i^{\rm scr} = -\alpha \frac{e^2 q_i}{S} \quad \text{and} \quad E_{\rm scr} = \frac{\beta}{2} \sum_i c_i q_i V_i^{\rm scr}. \qquad (1)$$

Here, e is the electron charge and S is the Wigner-Seitz (atomic sphere) radius. The q_i and c_i are, respectively, the average net charge (inside the atomic sphere) and the concentration for the ith alloy component. The screening parameters α and β were evaluated from supercell calculations using the locally self-consistent Green's function (LSGF) technique[28] in the work by Korzhavyi *et al.*[21] The values of β were found to vary linearly from $\beta = 1.00$ to 1.14, and those of α parameter to vary nonlinearly from $\alpha = 0.658$ to 0.830, as the alloy concentration changes from 0 to 100 at.% Cr. The CPA was also employed in this study for modeling the paramagnetic state of the Fe-Cr alloys within the disordered local-moment (DLM) approach.[29–31]

The total energies were calculated using the generalized gradient approximation[32,33] (GGA) within the full charge density (FCD) formalism.[34,35] All the self-consistent EMTO-CPA calculations were performed using an orbital momentum cutoff of $l_{\rm max} = 3$ for partial waves. The integration over the Brillouin zone was performed using a $37 \times 37 \times 37$ grid of special **k**-points determined according to the Monkhorst-Pack scheme.[36] For the calculations of electron density in the vicinity of the Fermi surface transition, a finer $47 \times 47 \times 47$ **k**-point grid was used. The core states were recalculated at each self-consistency iteration.

In addition to the EMTO-FCD calculations described above, we have performed the full potential projector augmented wave[37,38] (PAW) calculations of disordered Fe-rich alloys containing 6.25 and 12.5 at.% Cr, which were modeled using 256- and 128-atom supercells, respectively. The Vienna *ab initio* simulation package[39–41] (VASP) has been used for this purpose. The VASP-PAW calculations have been performed in the GGA.[42] The energy cutoff was 350 eV. The convergence criterion for the total energy was chosen to be 10^{-6} eV in the lattice parameter calculations and 10^{-8} eV in the elastic constants calculations. In order to keep the symmetry of the lattice, which is preserved on average in real macroscopic

alloys, the shape of the unit cells was kept fixed while all the atomic positions inside the supercell were relaxed until the forces acting on atoms were less than 10^{-2} eV/Å.

Both supercells were built up using a two-atom cubic unit cell of the bcc structure, translated $4 \times 4 \times 4$ times to form the 128-atom supercell and $4 \times 4 \times 8$ times to form the 256-atom supercell. Accordingly, we have used the $4 \times 4 \times 4$ Monkhorst-Pack k-point mesh in the case of the 128-atom supercell and the $4 \times 4 \times 2$ k-point mesh in the case of the 256-atom supercell. Convergence with respect to k points was checked by comparing the results for the equilibrium lattice constant and elastic moduli of the 128-atom supercell obtained using $2 \times 2 \times 2$ and $4 \times 4 \times 4k$-point meshes.

B. Elastic property calculations

A uniform lattice distortion in the elastic property calculations was imposed on the lattice by transforming the set of primitive vectors a_i to a set of new vectors a_i' using a strain tensor ε:

$$\begin{pmatrix} a_1' \\ a_2' \\ a_3' \end{pmatrix} = (\boldsymbol{I} + \varepsilon) \cdot \begin{pmatrix} a_1 \\ a_2 \\ a_3 \end{pmatrix}, \tag{2}$$

where I is the 3×3 identity matrix. There are 21 independent elastic constants C_{ij}, but symmetry of the cubic lattice reduces this number to only 3 independent constants (C_{11}, C_{12}, and C_{44}) for cubic lattices. A uniform isotropic straining (compression or expansion) of the lattice gives one the access to the bulk modulus B, which is a linear combination of two elastic constants

$$B = (C_{11} + 2C_{12})/3. \tag{3}$$

The bulk modulus for each alloy was evaluated using the calculated total energies as a function of Wigner-Seitz radius in the interval between 2.58 and 2.70 Bohr. The energy minimum was located using a fit to the Murnaghan equation of state[43,44]

$$E(V) = E(V_0) + \frac{B_0 V}{B_0'}\left(\frac{(V_0/V)^{B_0'}}{B_0' - 1} + 1\right) - \frac{B_0 V_0}{B_0' - 1}, \tag{4}$$

where V is the volume, B_0 and B_0' are the bulk modulus and its pressure derivative, respectively, at the equilibrium volume V_0.

In order to find all three cubic elastic constants, two more types of lattice strain should be considered. Following the procedure proposed by Mehl *et al.*,[45] we considered a volume-conserving orthorhombic strain

$$\varepsilon = \begin{pmatrix} x & 0 & 0 \\ 0 & -x & 0 \\ 0 & 0 & \frac{x^2}{1-x^2} \end{pmatrix} \tag{5}$$

for which the total energy is an even function of distortion x:

$$\Delta E(x) = \Delta E(-x) = V(C_{11} - C_{12})x^2 + O[x^4]. \tag{6}$$

The C_{44} elastic constant was calculated using a monoclinic volume-conserving strain

$$\varepsilon = \begin{pmatrix} 0 & \frac{x}{2} & 0 \\ \frac{x}{2} & 0 & 0 \\ 0 & 0 & \frac{x^2}{4-x^2} \end{pmatrix} \tag{7}$$

for which the total energy dependence has the form

$$\Delta E(x) = \Delta E(-x) = \tfrac{1}{2} V C_{44} x^2 + O[x^4]. \tag{8}$$

The value of distortion x was varied from zero (for the equilibrium state) to ± 0.05, in accordance with Mehl's prescription.[46] For each type of volume-conserving distortion, the calculated total energies were fitted by a parabola using x^2 as the variable. The values of elastic constants were obtained from the derivatives of ΔE with respect to x^2.

Once the single-crystal elastic constants are known, related properties of polycrystalline alloys may also be evaluated. A complication here is that, because of the elastic anisotropy, the Young modulus E and the shear modulus G of a cubic single crystal may depend on direction. The shear modulus anisotropy is usually expressed as the ratio between two elastic constants C_{44} and $C' = (C_{11} - C_{12})/2$:

$$A_G = \frac{2C_{44}}{C_{11} - C_{12}}. \tag{9}$$

There is no exact expression for the polycrystal-averaged shear modulus in terms of the C_{ij}, but one can evaluate approximate averages of the lower and upper bounds given by various theories.

The upper bound due to Voight[47] is calculated as

$$G_V = \frac{C_{11} - C_{12} + 3C_{44}}{5}, \tag{10}$$

and the lower bound due to Reuss[48] reads as

$$G_R = \frac{5(C_{11} - C_{12})C_{44}}{4C_{44} + 3(C_{11} - C_{12})}. \tag{11}$$

According to Hill,[49] the arithmetic average of the Voight and Reuss values can be used as an estimate of the average shear modulus

$$G = \frac{G_V + G_R}{2}. \tag{12}$$

Hashin and Shtrikman[50] have found that tighter bounds for G exist in the case of cubic crystals, namely,

$$G_1 = G_1^* + 3\Big/\left(\frac{5}{G_2^* - G_1^*} - 4\beta_1\right) \tag{13}$$

and

$$G_2 = G_2^* + 2\Big/\left(\frac{5}{G_1^* - G_2^*} - 6\beta_2\right). \tag{14}$$

Here,

$$\beta_1 = -\frac{3(B + 2G_1^*)}{5G_1^*(3B + 4G_1^*)}, \tag{15}$$

$$\beta_2 = -\frac{3(B + 2G_2^*)}{5G_2^*(3B + 4G_2^*)}, \tag{16}$$

$$G_1^* = \frac{C_{11} - C_{12}}{2},\ G_2^* = C_{44}, \tag{17}$$

and B is given by Eq. (3). The terms Hashin modulus (G_H) and Shtrikman modulus (G_S) are used, respectively, to denote the larger and the smaller of G_1 and G_2. By analogy with Eq. (12), we also made another estimate, the so-called

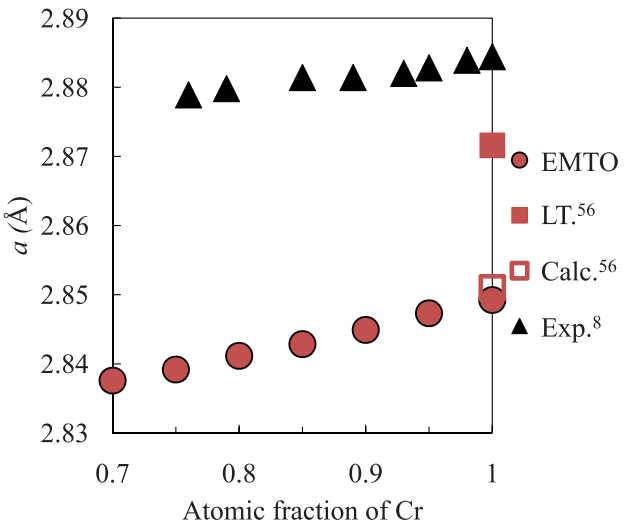

FIG. 1. (Color online) Lattice parameters of random bcc Fe-Cr alloys: Filled circles are the present EMTO-CPA results, an open square is the result of paramagnetic VASP-PAW calculations made in Ref. 56, a filled square is the low-temperature (LT) experimental lattice parameter used in the elastic constant calculations of Ref. 56 (the elastic constants are presented in Table I), and filled triangles are the experimental data from Ref. 8.

Hashin-Shtrikman average of the polycrystalline-averaged shear modulus, as

$$G = \frac{G_S + G_H}{2}. \tag{18}$$

Using either estimate of G,[51] one may evaluate the polycrystal-averaged Young's modulus

$$E = (9BG)/(3B + G)$$

and Poisson's ratio

$$\nu = (3B - E)/(6B).$$

III. RESULTS AND DISCUSSION

A. Elastic properties of Cr-rich alloys

Pure chromium and Cr-rich Fe-Cr alloys (with the iron content below 20 at.%) form different types of spin density wave (SDW) structures below the Néel temperature T_N, which has a maximum for pure Cr at 310 K. The magnetic phase transition has pronounced effects upon the elastic and other properties of Cr and its alloys.[4–7] However, this study is mostly concerned with the elastic properties in the *paramagnetic* state, which is modeled here using the DLM approach. Let us note that, according to the EMTO-CPA calculations in the paramagnetic DLM state, sizable magnetic moments remain on the Fe atoms, but disappear on the Cr atoms. As a result, DLM calculations for pure Cr in the paramagnetic state reduce to a nonmagnetic solution.[52,53]

For each alloy, we have calculated the elastic properties at the zero-Kelvin theoretical (GGA) equilibrium lattice parameter, as well as at the room-temperature experimental lattice parameter.[8,52,53] The experimental and theoretical lattice parameters used in the calculations are shown in Fig. 1. Although the lattice parameters calculated for the DLM state are lower than the experimental ones, the slope of concentration dependence is reproduced correctly by the EMTO-CPA calculations. In order to compare with the elastic constants that have been measured directly at 500 K,[7] we also calculate the elastic properties of Cr at the experimental lattice constant $a_{\rm exp}^{500} = 2.8935$ Å corresponding to that temperature.[8,9]

Let us note that the elastic moduli of pure Cr have been experimentally found to exhibit a pronounced nonmonotonic variation (a 30% drop in bulk modulus, for example) in a range of temperatures (±100 K) around the Néel temperature.[5] Such an extreme temperature dependence is a consequence of both the gradual and abrupt changes in the magnetic state of Cr, which can not be fully described using the theoretical techniques available to us. This circumstance should be kept in mind when making comparison between theoretical and experimental results for pure Cr or Cr-rich alloys.

Table I shows theoretically derived elastic properties of Cr in the paramagnetic state, calculated using several *ab initio* methods and at different lattice parameters, together with the experimental data from several sources.[4,6,7] In spite of

TABLE I. Theoretical and experimental single-crystal elastic constants C_{ij} (GPa), anisotropy constant A_G (dimensionless), and bulk modulus B (GPa) for pure Cr. The theoretical values have been obtained using nonmagnetic calculations employed to describe the paramagnetic state of pure Cr. The present EMTO calculations have been performed at the calculated theoretical lattice parameter, as well as at two experimental (Refs. 8 and 9) values of the lattice parameter corresponding to room temperature and 500 K. The paramagnetic VASP-PAW calculations Ref. 56 were done at a low-temperature lattice parameter value of 2.8792 Å (see text). The room-temperature experimental elastic constants reported in Ref. 7 were obtained by extrapolation of the elastic constants measured at high temperatures in order to exclude the contribution due to antiferromagnetic ordering. A similar extrapolation procedure was was carried out by Lenkkeri (Ref. 4) for the bulk modulus, and its result is shown in the last row (in parentheses), next to the directly measured room-temperature value.

Condition	C_{11}	C_{12}	C_{44}	C'	A_G	B
Calculated at $a_{\rm calc} = 2.8492$ Å[a]	484	140	105	172	0.61	255
Calculated at $a_{\rm exp}^{298} = 2.8844$ Å[a]	444	93	108	176	0.61	210
Calculated at $a_{\rm exp}^{500} = 2.8935$ Å[a]	431	83	89	174	0.51	199
Calculated at $a^{\rm LT} = 2.8792$ Å[b]	446	117	101	165	0.62	226
Measured at $T = 77$ K[c]	391	90	103	151	0.68	190
Measured at $T = 298$ K[c]	350	69	101	141	0.71	162
Measured at $T = 500$ K[c]	346	76	99	135	0.73	166
Measured at $T = 150$ K[d]	375	85	101	145	0.69	182
Extrapolated to $T = 298$ K[d]	388	103	101	143	0.70	198
Measured at $T = 500$ K[d]	373	103	98	135	0.73	193
Measured at $T = 295$ K[e]						166(201)

[a]EMTO calculations (this paper).
[b]VASP-PAW calculations (Ref. 56).
[c]Experiment, ultrasonic resonance technique (Ref. 6).
[d]Experiment, ultrasonic phase comparison method (Ref. 7).
[e]Experiment, ultrasonic pulse-echo overlap method (Ref. 4).

the difficulty mentioned above, one can see that agreement between theoretical and experimental data is fair for most of the elastic properties, except the elastic constants C' and C_{11}, the theoretical values of which seem to be a bit higher than the measured or extrapolated experimental values corresponding to the paramagnetic state. Although we do not exactly know the cause of this discrepancy, most probably it indicates that our theoretical treatment of the paramagnetic state of Cr is too simple.

Let us note that even experimental results are quite scattered. In particular, the data by Bolef and de Klerk[6] show the largest deviation from our theoretical results, as well as from the rest of experimental data. As discussed by Katahara *et al.*,[7] the deviation could be related to the preparation details of the specimens. Another source of confusion has been the experimental room-temperature value of the lattice parameter of chromium reported by Straumanis and Weng to be 2.87918 kX units,[54] but quoted and used by Bolef and de Klerk[6] as if it were expressed in angstrom units, without actually applying the conversion factor 1.00202 Å/kX.[55] The same numerical value of experimental lattice parameter was then erroneously used in the elastic constant calculations of Ref. 56. Nevertheless, since that value of the lattice parameter is rather close to the true experimental value for pure Cr at very low temperatures, one can interpret the results of Ref. 56 as corresponding to low-temperature paramagnetic chromium. Hereafter (e.g., in Table I), this value of lattice parameter is referred to as a^{LT}.

We have investigated the elastic properties of Cr-rich Fe-Cr alloys, using the EMTO-CPA calculations described above, at the 0-K calculated lattice parameter a_{calc} as well as at the room-temperature experimental[8] lattice parameter a_{exp}^{298} (see Table I for numerical values for pure Cr). The dependence of the elastic properties on the lattice parameter is calculated to be rather weak. Therefore, the results obtained at the theoretical 0-K lattice parameter a_{calc} are shown in Fig. 2 (empty symbols connected by dashed lines) only for the bulk and the shear moduli, as well as for Poisson's ratio, the values of which are found to be most sensitive to the lattice parameter. The rest of the theoretical data shown in Fig. 2 (filled symbols connected by solid lines) have been calculated at the experimental lattice parameter a_{exp}^{298}.

In Fig. 2(a), the calculated elastic (bulk, Young's, and shear) moduli of paramagnetic Cr-rich Fe-Cr alloys are compared with the room-temperature experimental values from Refs. 4 and 5. Let us note that directly measured experimental data are plotted for the alloys, whereas the experimental data shown for pure chromium have been obtained by extrapolation from high temperatures to room temperature, as discussed above and described in Refs. 4 and 7. This is so because the addition of Fe to Cr very efficiently suppresses the critical temperature of magnetic ordering, so the alloys are in the paramagnetic state already at room temperature.

As one can see from Fig. 2(a), the concentration dependence of the bulk modulus is almost linear. The Young's and the shear moduli also exhibit linear dependencies on concentration, deflecting slightly from a straight line only very close to pure Cr. The bulk modulus is very sensitive to the lattice expansion: it changes by about 45 GPa between the 0-K calculated and the room-temperature experimental lattice parameters, whereas

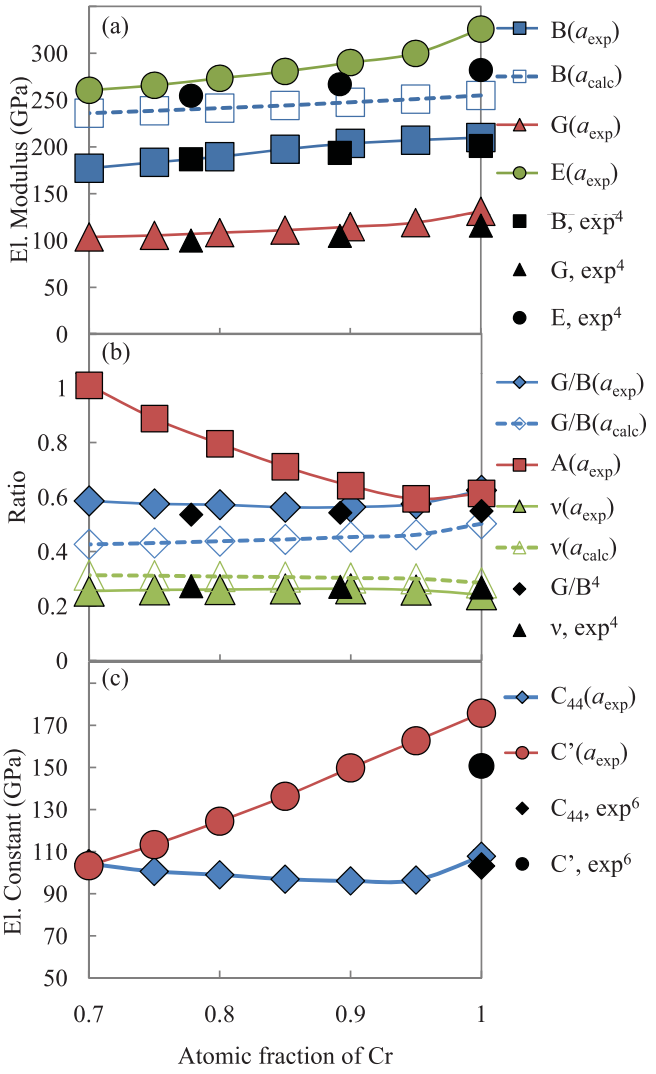

FIG. 2. (Color online) Calculated and experimental elastic properties of Cr-rich Fe-Cr alloys: (a) bulk modulus B, Young's modulus E, and shear modulus G (GPa); (b) Poisson's rato ν, anisotropy constant A_G, and G/B ratio (dimensionless); (c) calculated single-crystal elastic constants C_{44} and C' (GPa). The elastic properties have been calculated, using the DLM model of paramagnetic state of the alloys, at the room-temperature experimental lattice parameters (Ref. 8) (filled symbols connected by solid lines) and, for the properties sensitive to volume, also at the theoretical equilibrium lattice parameter a_{calc} (empty symbols connected by dashed lines). Experimental data from Refs. 4 and 6 for paramagnetic Cr and Fe-Cr alloys are shown for comparison (black symbols).

the E and G remain practically the same in this interval of lattice parameters. The best agreement with experimental data for the bulk modulus is obtained when it is calculated at the lattice parameter of the experiment.

Figure 2(b) shows Poisson's ratio ν, anisotropy constant A_G, and G/B ratio as a function of composition for Cr-rich Fe-Cr alloys. A difference of about 0.05 is obtained between the values of Poisson's ratio calculated at the 0-K theoretical and the room-temperature experimental lattice parameters. Figure 2(c) shows the calculated shear elastic constants C_{44} and C' as functions of concentration. The two concentration

dependencies are linear but have different slopes, so that they cross at a concentration of about 30 at.% Fe. At the same alloy composition, the anisotropy constant A_G becomes equal to one, indicating that elastic properties of the alloy are isotropic. The anisotropy constant in the Cr-rich alloys changes nonlinearly close to pure Cr and exhibits a minimum at 5 at.% Fe. A strong concentration dependence of elastic anisotropy, as well a difference in elastic properties between the matrix and the precipitate phases (formed, for instance, as a result of spinodal decomposition), may cause changes in strain contrast from the precipitates, which may be utilized in transmission electron microscopy studies for identification and discrimination of Cr-rich areas having different Fe content.

In order to evaluate the expected brittleness or ductility of Fe-Cr alloys, we have also calculated the ratio of shear modulus to bulk modulus G/B, as proposed by Pugh.[57] For ductile materials, this ratio is typically smaller than 0.5; materials having higher values of the ratio tend to exhibit brittle behavior. The calculated G/B ratio for Fe-Cr alloys is found to vary from 0.61 for pure Cr to 0.59 for $Cr_{70}Fe_{30}$. Thus, according to this criterion, Fe-Cr alloys are expected to exhibit brittle behavior in the investigated compositional range of Cr-rich Fe-Cr alloys (0–30 at.% Fe).

B. Elastic properties of Fe-rich alloys

In contrast to the Cr-rich Fe-Cr alloys, the Fe-rich alloys (0–20 at.% Cr) are in the ferromagnetic state at temperatures below 800–1000 K. Therefore, thermal magnetic excitations do not make a significant contribution to the elastic properties of the alloys at room temperature. Thus, in this case, our calculations have been carried out for the ferromagnetic state and at two different sets of lattice parameters: (i) room-temperature experimental lattice parameters from Refs. 8 and 9, and (ii) theoretical equilibrium lattice parameters as obtained from the present EMTO-CPA calculations. The main reason for presenting here these two sets of results is to illustrate the sensitivity of some elastic moduli (bulk modulus, for example) to lattice parameter. In addition, as will be discussed below, there exists an unresolved issue about the difference between theoretical and experimental concentration dependencies of the lattice parameter in Fe-rich Fe-Cr alloys.

The calculated and experimental lattice parameters are shown in Fig. 3. First, the upper panel of the figure shows that the room-temperature experimental lattice parameters are noticeably higher than the theoretical ones calculated at zero Kelvin. Let us note that this difference is mainly due to the errors in the description of the exchange correlation part of the GGA total energy functional rather than due to thermal expansion. Indeed, a zero-temperature limit (zero-point vibrations removed) of the experimental lattice parameter for pure Fe is 2.853 Å,[58] while the corresponding theoretical values are noticeably smaller: 2.837 Å (EMTO), 2.833 Å [full-potential linearized augmented plane-wave plus local-orbitals method (Ref. 58)], and 2.832 Å [VASP-PAW (this paper)].

Second, one can see from the lower panel of Fig. 3 (where the difference between the lattice spacing in the alloy and that in pure Fe is plotted) that the zero-temperature theoretical and the room-temperature experimental lattice parameters exhibit

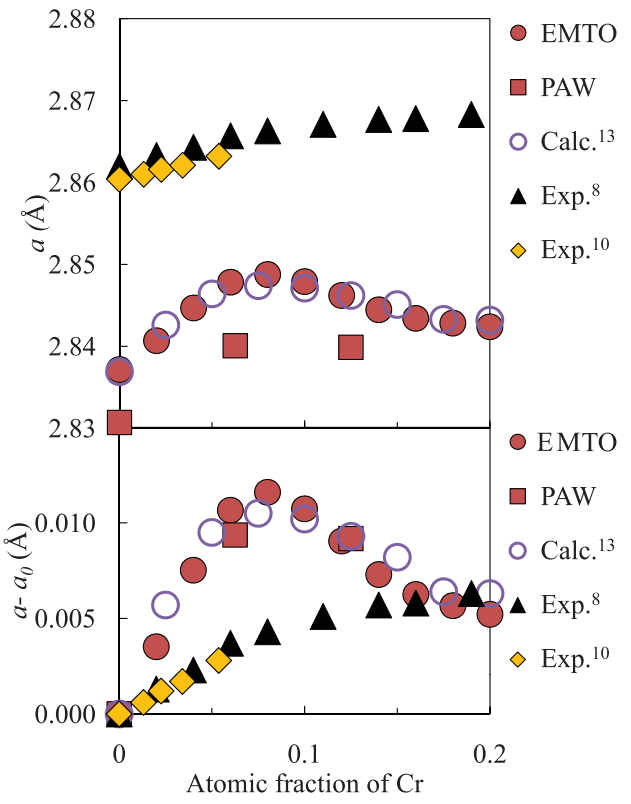

FIG. 3. (Color online) Lattice parameter of disordered bcc Fe-Cr alloys (upper panel) and that relative to the lattice parameter of pure Fe (lower panel). The EMTO-CPA and VASP-PAW results are shown by filled circles and squares, respectively. Empty circles denote the theoretical EMTO-CPA results of Ref. 13. The experimental data from Refs. 10 and 8 are given by filled diamonds and triangles, respectively.

substantially different concentration dependencies. In particular, the theory (0 K) predicts the existence of a pronounced maximum at about 7 at.% Cr. The maximum has also been obtained in previous theoretical investigations.[13,20,21] Although this and the previous calculations have been performed using the CPA, their results are in very good agreement with the present VASP-PAW calculations using supercells in which the local-relaxation and the local-environment effects (that are neglected in the CPA) have been taken into consideration. The origin of the lattice parameter anomaly obtained in all the calculations (but absent in the experimental data) is still unclear and deserves a separate investigation.

In order to demonstrate the volume dependence of the elastic properties, we show in Fig. 4 the concentration dependencies of the bulk modulus B and elastic constants C_{44} and C', calculated at the experimental and theoretical equilibrium lattice parameters that are shown in Fig. 3. One can clearly see the difference between two sets of results for the bulk modulus, while the effect of lattice spacing on the C_{44} and C' elastic constants is rather modest. It is also clear that the use of experimental lattice parameter in the calculations provides good agreement between theory and experiment for the bulk modulus.

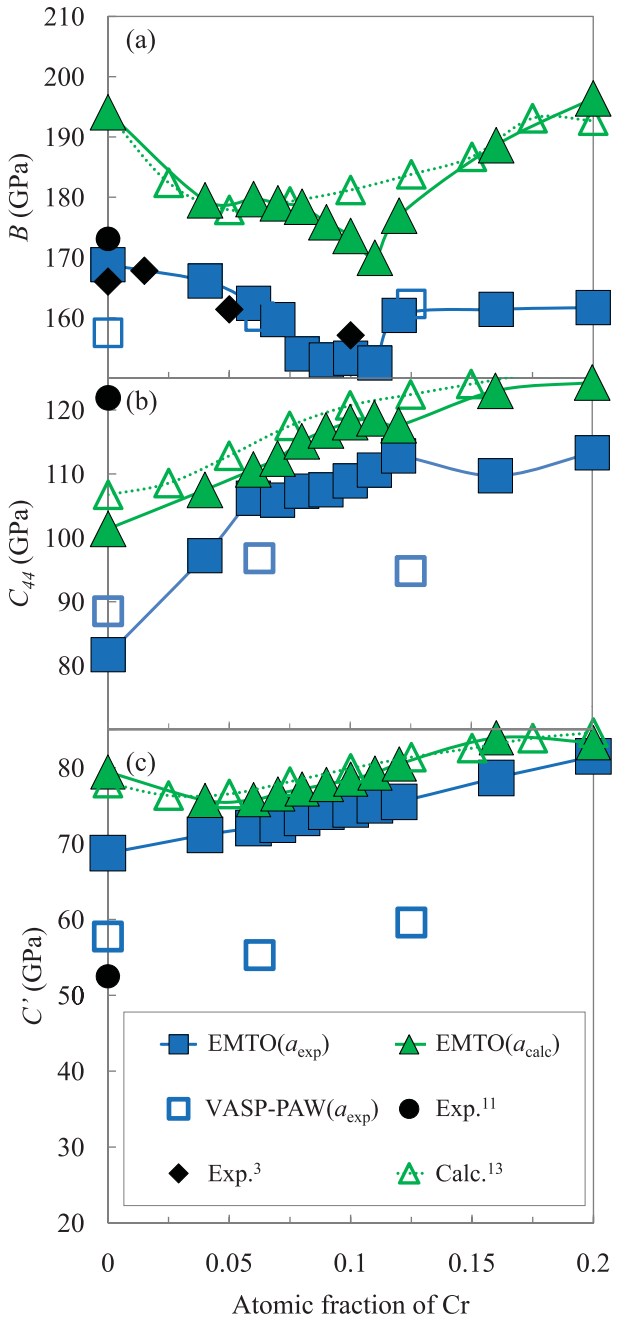

FIG. 4. (Color online) (a) Bulk modulus B, and shear elastic constants (b) C_{44} and (c) C' calculated using EMTO-CPA and VASP-PAW methods at experimental and theoretical lattice parameters. Experimental data are from Refs. 3 and 11. The results are also compared with previous EMTO-CPA calculations of Ref. 13. The legend applies to all panels.

Another important point is to compare the results of the present and previous EMTO-CPA calculations of elastic properties with the results of VASP-PAW calculations of elastic properties for pure Fe as well as for Fe-Cr alloys. We note, in passing, that substitutionally disordered alloys are treated completely differently by these two methods. If the EMTO-CPA is a single-site mean-field theory of electronic structure of random alloys, where the so-called local-environment effects are neglected, the VASP-PAW calculations employ large supercells in order to model the distribution of atoms in random alloys. The supercell approach is supposed to be more accurate, provided that the results have been converged with respect to supercell size and other parameters of the method such as the number of k points. Since such calculations are too cumbersome, we can only conclude that there is reasonable qualitative agreement between the two approaches.

Quantitatively, the results obtained using the two methods differ as much as by 20% for C_{44}. The best agreement between the two methods is obtained for the bulk modulus, which is quite expectable, since the EMTO is supposed to be very accurate in the case of a homogeneous lattice distortion. In Fig. 5, we show the calculated and experimentally measured values of Young's modulus E, shear modulus G, anisotropy constant A_G, and G/B ratio. It is clear that the VASP-PAW results are in much better agreement with experimental data than the EMTO-CPA results. The averaged absolute difference between the elastic constants calculated using VASP-PAW and EMTO-CPA is 8 GPa for pure Fe or for the Fe 6.25 at.% Cr alloy, and 9 GPa for the alloy with 12.5 at.% Cr. Apparently, more tests should be done, but this goes beyond the scope of this paper.

Let us now turn to concentration dependencies of the elastic properties. As Fig. 4 clearly shows, the calculated concentration dependence of the bulk modulus and that of the C_{44} elastic constant exhibit peculiarities in a narrow concentration range between 8 and 12 at.% Cr. The experimental data by Speich *et al.*[3] seem to indicate a similar behavior of the bulk modulus to the one calculated in this paper, although the amount of experimental information is insufficient for a detailed description of the concentration dependence in the region of interest. The peculiarity in the calculated properties may be ascribed to the so-called electronic topological transition (ETT), caused by the changes of the Fermi surface topology near this concentration, as reported in Ref. 21. According to the theory of ETT,[59–64] higher-order derivatives of the thermodynamic potential, such as the elastic properties (second derivatives), may exhibit anomalies (kinks) near the concentrations where the topology of the Fermi surface of alloys undergoes an abrupt change. The ETT reported for several systems was reviewed in Ref. 63. For instance, Abrikosov *et al.*[61] and Korzhavyi *et al.*[64] predicted such anomalies in the bulk modulus and in the Grüneisen constant of Li-Mg and Al-Li alloys near the ETT concentrations; Hacinskaya *et al.*[63] found a prominent peak in the computed bulk modulus as well as in the thermal expansion coefficient of Ni-W alloys at the ETT concentration.

In Figs. 4 and 5, we also show (open symbols connected by dashed lines) the elastic properties of Fe-Cr alloys calculated recently by Zhang *et al.*[13] By using a similar EMTO-CPA technique, they found a shallow local minimum in the bulk modulus at about 5 at.% Cr. As discussed in this paper, this minimum may be traced back to the excess lattice expansion (caused by the maximum in the calculated concentration dependence of the lattice parameter) at these alloy concentrations. The results reported by Zhang *et al.* are in close agreement with ours. However, Zhang *et al.* did not find the peculiarities in the elastic properties close near 10 at.% Cr. This is, most probably, due to the large step of the concentration grid used

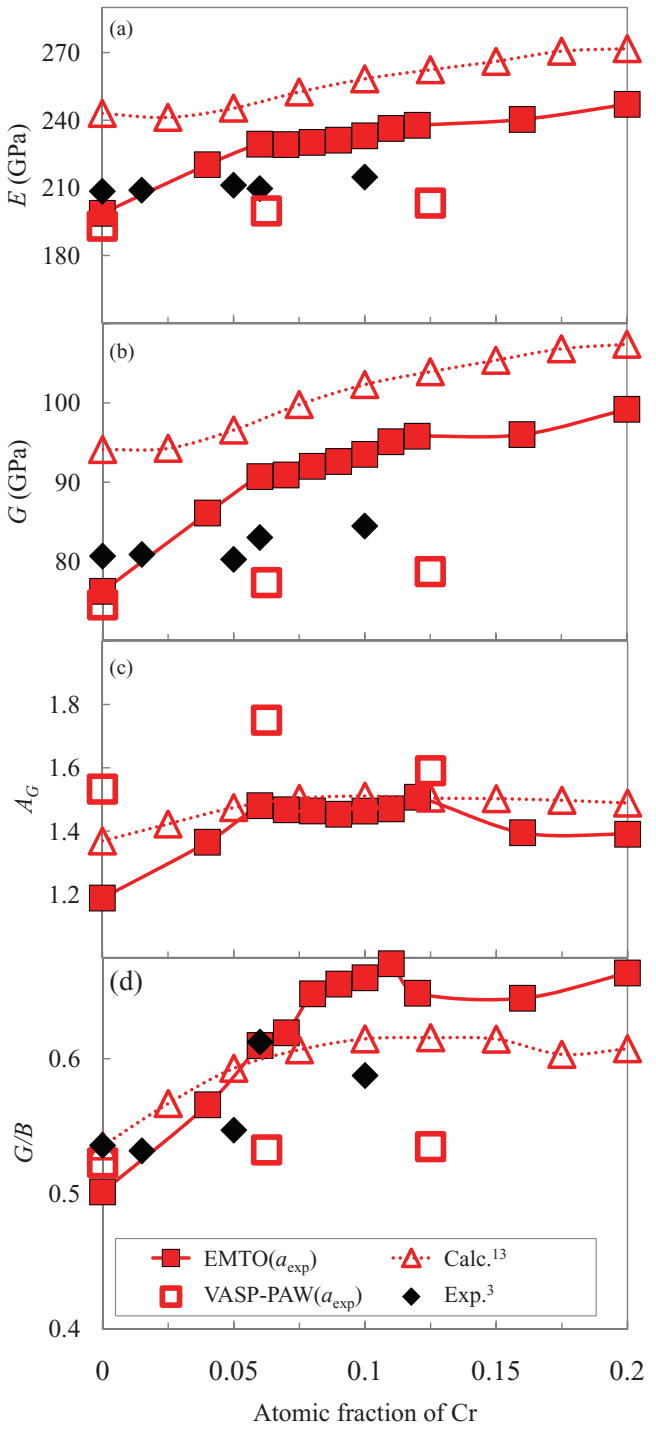

FIG. 5. (Color online) Young's modulus E, shear modulus G, anisotropy constant A_G, and G/B ratio calculated for the experimental and theoretical lattice parameters by the EMTO-CPA and VASP-PAW methods. Experimental data are from Ref. 3. The results are also compared with previous EMTO-CPA calculations of Ref. 13. The legend applies to all panels.

in their study. Also, for the kind of anomalies dealt with in the present study, the density of k-point mesh is a crucial parameter.

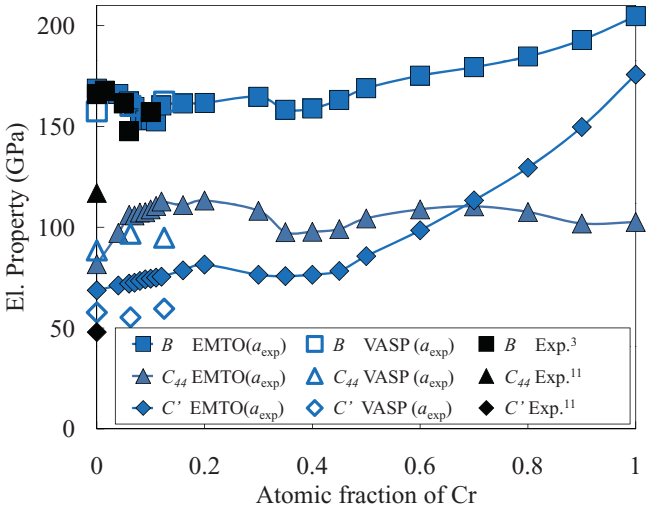

FIG. 6. (Color online) Bulk modulus B, elastic constants C_{44} and C' calculated in the FM state for the experimental lattice parameters by the EMTO-CPA and VASP-PAW methods for the whole compositional range. Experimental data are from Refs. 3 and 11.

Finally, Fig. 6 presents the calculated and experimental elastic properties of random Fe-Cr alloys (in the FM state) for the whole range of alloy compositions. One can see that the properties exhibit nonmonotonic behavior around a composition of 40 at.% Cr. One possible reason for this peculiar behavior is the disappearance of local magnetic moments on Cr atoms near this composition (see Ref. 21).

IV. CONCLUSIONS

Elastic properties of disordered Cr- and Fe-rich Fe-Cr binary alloys have been calculated by the EMTO-CPA and supercell VASP-PAW method. Good agreement with available experimental data is found for all calculations. A peculiarity in the elastic properties is found and related to the changes of Fermi surface topology occurring in the Fe-rich region at 8–12 at.% Cr according to our calculations. The calculations predict rather high values for the elastic moduli of Cr-rich alloys containing up to 30 at.% of Fe, without any peculiarities in their almost linear concentration dependencies in that region. However, these alloys may be expected to be rather brittle according to the Pugh criterion (G/B ratio).

ACKNOWLEDGMENTS

Computer resources for this study have been provided by the Swedish National Allocation Committee (SNAC) at the National Supercomputer Center (NSC), Linköping. This work was performed within the VINNEX center Hero-m, financed by the Swedish Governmental Agency for Innovation Systems (VINNOVA), Swedish industry, and the Royal Institute of Technology (KTH). This study was partly financed with grants from Jernkontoret, the European Research Council, and the Swedish Research Council. P.A.K. acknowledges financial support from SKB, the Swedish Nuclear Fuel and Waste Management Company.

*razvsevol@yahoo.com

[1] I. Cook, Nat. Mater. **5**, 77 (2006).

[2] *Binary Alloy Phase Diagrams*, 2nd ed., edited by T. B. Massalski (ASM International, Materials Park, Ohio, 1990), pp. 1271–1273.

[3] G. R. Speich, A. J. Schwoeble, and W. C. Leslie, Metall. Trans. **3**, 2031 (1972).

[4] J. T. Lenkkeri, J. Phys. F: Met. Phys. **10**, 611 (1980).

[5] E. E. Lähteenkorva and J. T. Lenkkeri, J. Phys. F: Met. Phys. **11**, 767 (1981).

[6] D. I. Bolef and J. de Klerk, Phys. Rev. **129**, 1063 (1963).

[7] K. W. Katahara, J. Phys. F: Met. Phys. **9**, 2167 (1979).

[8] G. D. Preston, Philos. Mag. **13**, 419 (1932).

[9] G. K. White, R. B. Roberts, and E. Fawcett, J. Phys. F: Met. Phys. **16**, 449 (1986).

[10] A. L. Sutton and W. Hume-Rothery, Philos. Mag. **46**, 1295 (1955).

[11] J. A. Rayne and B. S. Chandrasekhar, Phys. Rev. **122**, 1714 (1961).

[12] D. J. Dever, J. Appl. Phys. **43**, 3293 (1972).

[13] H. Zhang, B. Johansson, and L. Vitos, Phys. Rev. B **79**, 224201 (2009).

[14] G. Y. Guo and H. H. Wang, Chin. J. Phys. **38**, 949 (2000).

[15] L. Vocadlo, G. A. de Wijs, G. Kresse, M. Gillan, and G. D. Price, Faraday Discuss. **106**, 205 (1997).

[16] K. J. Caspersen, A. Lew, M. Ortiz, and E. A. Carter, Phys. Rev. Lett. **93**, 115501 (2004).

[17] P. Söderlind, R. Ahuja, O. Eriksson, J. M. Wills, and B. Johansson, Phys. Rev. B **50**, 5918 (1994).

[18] X. W. Sha and R. E. Cohen, Phys. Rev. B **74**, 214111 (2006).

[19] E. Fawcett, H. L. Alberts, V. Yu. Galkin, D. R. Noakes, and J. V. Yakhmi, Rev. Mod. Phys. **66**, 25 (1994).

[20] P. Olsson, I. Abrikosov, L. Vitos, and J. Wallenius, J. Nucl. Mater. **321**, 84 (2003).

[21] P. A. Korzhavyi, A. V. Ruban, J. Odqvist, J.-O. Nilsson, and B. Johansson, Phys. Rev. B **79**, 054202 (2009).

[22] P. Hohenberg and W. Kohn, Phys. Rev. **136**, B864 (1964).

[23] L. Vitos, H. L. Skriver, B. Johansson, and J. Kollar, Comput. Mater. Sci. **18**, 24 (2000).

[24] L. Vitos, Phys. Rev. B **64**, 014107 (2001).

[25] L. Vitos, I. A. Abrikosov, and B. Johansson, Phys. Rev. Lett. **87**, 156401 (2001).

[26] B. L. Gyorffy, Phys. Rev. B **5**, 2382 (1972).

[27] A. V. Ruban and H. L. Skriver, Phys. Rev. B **66**, 024201 (2002); A. V. Ruban, S. I. Simak, P. A. Korzhavyi, and H. L. Skriver, *ibid.* **66**, 024202 (2002).

[28] I. A. Abrikosov, A. M. N. Niklasson, S. I. Simak, B. Johansson, A. V. Ruban, and H. L. Skriver, Phys. Rev. Lett. **76**, 4203 (1996); I. A. Abrikosov, S. I. Simak, B. Johansson, A. V. Ruban, and H. L. Skriver, Phys. Rev. B **56**, 9319 (1997).

[29] B. L. Gyorffy, A. J. Pindor, J. B. Staunton, G. M. Stocks, and H. Winter, J. Phys. F: Met. Phys. **15**, 1337 (1985).

[30] B. L. Gyorffy, A. J. Pindor, G. M. Stocks, and H. Winter, J. Magn. Magn. Mater. **45**, 15 (1984).

[31] A. V. Ruban, P. A. Korzhavyi, and B. Johansson, Phys. Rev. B **77**, 094436 (2008).

[32] Y. Wang and J. P. Perdew, Phys. Rev. B **44**, 13298 (1991).

[33] J. P. Perdew, J. A. Chevary, S. H. Vosko, K. A. Jackson, M. R. Pederson, D. J. Singh, and C. Fiolhais, Phys. Rev. B **46**, 6671 (1992).

[34] L. Vitos, *Computational Quantum Mechanics for Materials Engineers* (Springer-Verlag, London, 2007).

[35] L. Vitos, I. A. Abrikosov, and B. Johansson, Phys. Rev. Lett. **87**, 156401 (2001).

[36] H. J. Monkhorst and J. D. Pack, Phys. Rev. B **13**, 5188 (1972).

[37] P. E. Blöchl, Phys. Rev. B **50**, 17953 (1994).

[38] G. Kresse and D. Joubert, Phys. Rev. B **59**, 1758 (1999).

[39] G. Kresse and J. Hafner, Phys. Rev. B **47**, 558 (1993).

[40] G. Kresse and J. Hafner, Phys. Rev. B **49**, 14251 (1994).

[41] G. Kresse and J. Furthmuller, Phys. Rev. B **54**, 11169 (1996).

[42] J. P. Perdew, K. Burke, and Y. Wang, Phys. Rev. B **54**, 16533 (1996).

[43] C. L. Fu and K. M. Ho, Phys. Rev. B **28**, 5480 (1983).

[44] F. D. Murnaghan, Proc. Natl. Acad. Sci. USA **30**, 244 (1944).

[45] M. J. Mehl, B. M. Klein, and D. A. Papaconstantopoulos, in *Intermetallic Compounds: Principles and Practice, Volume I Principles*, edited by J. H. Westbrook and R. L. Fleischer (Wiley, London, 1995), pp. 195–210.

[46] M. J. Mehl, Phys. Rev. B **47**, 2493 (1993).

[47] W. Voigt, Ann. Phys. (Leipzig) **38**, 573 (1889).

[48] A. Reuss, Z. Angew. Math. Mech. **9**, 49 (1929).

[49] R. Hill, Proc. Phys. Soc., London, Sect. A **65**, 349 (1952).

[50] Z. Hashin and S. Shtrikman, J. Mech. Phys. Solids **10**, 343 (1962).

[51] We find that the anisotropy of shear modulus in Fe-Cr alloys is relatively weak. As a result, the two estimates of polycrystalline-averaged shear modulus given by Eqs. (12) and (18) are almost equal to each other for the Cr-rich alloys. For example, for pure Cr, the former estimate (Hill average) is 127.9 GPa and the latter one (Hashin-Strikman average) is 126.9 GPa. For $Fe_{10}Cr_{90}$, the estimates are 124.3 and 124.1 GPa, respectively. As soon as there is no significant difference between the Hashin-Shtrikman and the Hill averages for the present alloy system, in the following only the values of G calculated as the Hill average, Eq. (12), are given. We note here that a similar conclusion may be drawn about the Fe-rich alloys in the ferromagnetic state; we will use the Hill average to estimate polycrystalline-averaged elastic moduli of these alloys, as well.

[52] V. I. Razumovskiy, E. I. Isaev, A. V. Ruban, and P. A. Korzhavyi, Intermetallics **16**, 982 (2008).

[53] V. I. Razumovskiy, E. I. Isaev, A. V. Ruban, and P. A. Korzhavyi, Mater. Res. Soc. Symp. Proc. **1128**, U05-28 (2009).

[54] M. E. Straumanis and C. C. Weng, Acta Crystallogr. **8**, 367 (1955).

[55] W. L. Bragg, J. Sci. Instrum. **24**, 27 (1947).

[56] Application Note: Chromium: Structure and Elastic Properties, Materials Design, Inc. 2002–2008 [http://www.materialsdesign.com].

[57] S. F. Pugh, Philos. Mag. **45**, 823 (1954).

[58] P. Haas, F. Tran, and P. Blaha, Phys. Rev. B **79**, 085104 (2009).

[59] I. M. Lifshitz, Zh. Eksp. Teor. Fiz. **38**, 1569 (1960) [Sov. Phys. JETP **11**, 1130 (1960)].

[60] V. G. Vaks and A. V. Trefilov, J. Phys. F: Met. Phys. **18**, 213 (1988).

[61] I. A. Abrikosov, Yu. H. Vekilov, P. A. Korzhavyi, A. V. Ruban, and L. E. Shilkrot, Solid State Commun. **83**, 867 (1992).

[62] Ya. M. Blanter, M. I. Kaganov, A. V. Pantsulaya, and A. A. Varlamov, Phys. Rep. **245**, 159 (1994).

[63] E. Bruno, B. Ginatempo, E. S. Giuliano, A. V. Ruban, and Yu. Kh. Vekilov, Phys. Rep. **249**, 353 (1994).

[64] P. A. Korzhavyi, A. V. Ruban, S. I. Simak, and Yu. Kh. Vekilov, Phys. Rev. B **49**, 14229 (1994).